sciendo
ISSN 1335-8871
MEASUREMENT SCIENCE REVIEW
Journal homepage: https://content.sciendo.com

Measurement and Evaluation of Insulating Properties of a Modified Dielectric Surface using Plasma Discharge

Roman Pernica, Miloš Klima, Pavel Fiala*

Department of Theoretical and Experimental Electrical Engineering, Brno University of Technology, Technicka 3082/12, 616 00 Brno, Czech Republic, 15788@vut.cz, klimam@vut.cz, fialap@vut.cz

Abstract: Plasma discharges under atmospheric pressure can be used to modify the electrical properties of metallic and dielectric surfaces. The aim of such a modification is to achieve an improvement in the characteristic parameters of the surface, for example in the area of the electrical strength of the surface, in order to achieve a higher ultimate level of electrical breakdown E_b when tested with pulsed or alternating electrical voltages. So far, research has focused on a set of functional experiments carried out using plasma on samples of two types of dielectric materials (thermoset, thermoplastic) with an impact on the final effect of the level of electrical breakdown voltage, electrical intensity and E_b. surface conductivity. The treatment technology requires repeatability and consideration of the industrial deployment conditions of plasma technology. The surface structure was modified in a defined and repeatable way by plasma discharge under atmospheric pressure without the presence of precursors. Methods to evaluate these modifications assessed the change in parameters related to sample type, repeatability and prediction of treatment stability. Subsequently, the surface strength of both the modified samples and the samples not affected by the plasma discharge was measured.

Keywords: Plasma, treatment, dielectric, electrical strength, numerical model, precursor, nanosurface, HV apparatus.

1. INTRODUCTION

In surface treatment technology, plasma discharge treatment [1] is used to adjust the parameters of the upper layers of material surfaces. It is performed on various changes of surface properties at the molecular and atomic level [2]. The treatment technology uses physical or chemical changes of the target material by specially generated plasma using specially designed generators [3] under repeatable, predefined conditions. The vacuum technology of plasma-enhanced chemical vapor deposition (PECVD) is frequently used. However, high-frequency discharge generators to produce plasma at atmospheric pressure are also expanding. These technologies have several advantages over vacuum applications.

Methods for generating non-thermal high-frequency plasma discharges have been introduced in industry and have application potential [4]-[5]. The technology is well known and is used in the field of thin film deposition [6] and surface modifications. The advantage of using plasma discharges under atmospheric pressure is that local structures can be easily generated with the supplied precursors [7]. The electromagnetohydrodynamics (EMHD) [1] of plasma discharges depends on the parameters of the electrical generator and the chamber that excites the plasma [8]-[10]. A simple chamber arrangement can include a device that uses a central RF electrode and an argon atmosphere [7] to form a generator system (kINPen). This approach has been used for the generation of COST microplasma current in He [8] and the use of an RF plasma pencil for plasma generation [9]. Furthermore, this method was supported by parallel RF and grounded electrodes [8] and the RF plasma pencil.

The plasma generators contain an electrical generator and a high-frequency electrode system with an operating frequency of $f = 13.56$ MHz. When the generator system is in operation, an atmosphere composed of argon, nitrogen and other gases flows through the chamber, either independently or with the addition of precursor gases or substances [9]. The electromagnetic discharge parameters are determined by the geometrical arrangement of the chamber, the electrodes, the shape of the excitation signal of the RF generator and other related parameters [10]-[12].

2. SURFACE STRENGTH OF INSULATORS

Due to the development in the design and manufacture of HV and MV devices [13]-[15] and equipment [16]-[17], [19], one of the studied product parameters is the ability to withstand the effect of electrical surges. This parameter is tested using two methods. The first is a shock wave, the

DOI: 10.2478/msr-2024-0029

*Corresponding author: fialap@vut.cz (P. Fiala)

second test is a harmonic electric voltage (f = 50 or 60 Hz) for a duration of t_{test} = 1 s in accordance with the corresponding recommendations of the relevant standards. During this test (pulse or harmonic voltage waveform for t_{test} = 1 s), an electrical breakdown may occur in the device or on its surface through the volume of the insulator or at the interface of the insulator (dielectric/metal, dielectric/dielectric), Fig. 1. The tests are repeated to ensure the stability of the measured parameters.

Research into the electrical strength (E_b) of the product (breakdown parameters) during testing is important for equipment design and material selection, modification and assembly technology. The aim is to find a repeatable manufacturing process and to achieve the maximum electric field strength E_p during the prescribed and performed tests ($E_p = E_b$), and thus ensure the safety of the equipment during its operation, especially at the insulator interface (Fig. 1).

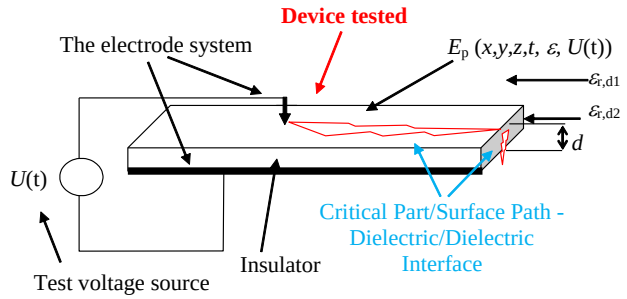

Fig. 1. The principle of the HV test for the surface electric field intensity E_p [V/m] of the proposed device.

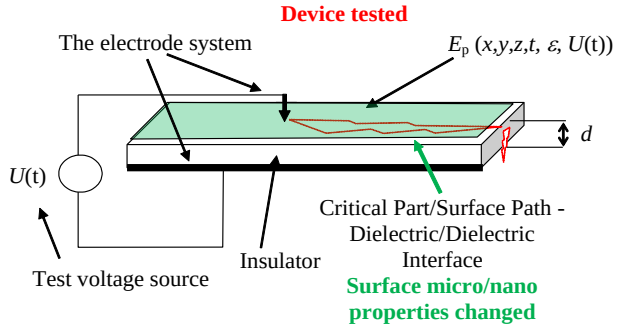

Fig. 2. Increase of the surface electric field intensity E_p of the proposed device by changing the micro/nano surface properties of the insulator.

The low values achieved in the E_p electric field intensity tests and the repeatability of the HV test parameters have so far been addressed by standard "macroscopic" methods:

1. Designing a longer electric field intensity E_p jump path (Fig. 1), distance d or surface shape modifications (Fig. 3).
2. Designing changes in the electric breakdown conditions of the electric field intensity E_p (Fig. 1), and changing the surface properties while maintaining the distance d by adjusting the micro/nano surface properties [20], Fig. 2.

Testing the surface properties of dielectric materials is defined in published standards. Schematically, this method could be expressed as the determination of the values of breakdown stress U_d and breakdown intensity E_b, according to the configuration in Fig. 3. Based on traditional experience from empirical measurements [21], an approximate relationship between bulk and surface electric strength can be established by the expression:

$$\frac{E_{pn,\varepsilon}}{E_{pt,\varepsilon}} = \frac{100 \cdot 10^3}{300} = \frac{1}{3}\ 10^3 \tag{1}$$

where $E_{pn,\varepsilon}$ is the electric field intensity in the normal direction of a material with the relative permittivity ε_r, and $E_{pt,\varepsilon}$ is the electric field intensity in the tangential direction. The standard design of the interface shapes and dimensions of the insulation materials of the device under test then encounters critical parameters, and the key factor is expressed by the formula:

$$\frac{a}{b} = \frac{\varepsilon_{r,d2}}{\varepsilon_{r,d1}} \tag{2}$$

where a, b are the distances and dimensions of the dielectric shaping, $\varepsilon_{r,d1}$ is the relative permittivity of the surrounding dielectric (air), $\varepsilon_{r,d2}$ is the relative permittivity of the dielectric (insulator material), according to Fig. 3.

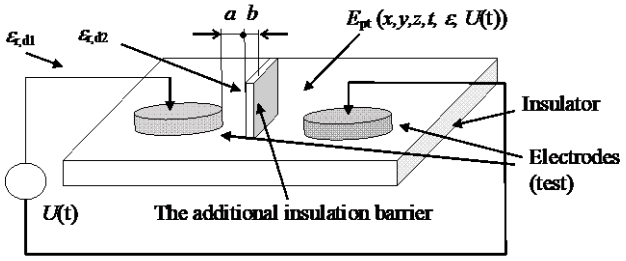

Fig. 3. The principal arrangement electrodes and dielectrics for measuring the surface electrical strength E_b [V/m].

One of the progressive methods for increasing the surface electric field intensity of E_p in the development of a particular device is the use of microscopic (nanoscopic) modifications of the surface of the dielectric/dielectric interface. Surface modification techniques such as sandblasting are known to allow microscopic modifications of surface properties [15]-[17]. Another progressive method is the modification/ deposition of a nanosurface on a dielectric to increase the surface electric field intensity value E_p. In this context, the effects of residual electric charges σ [C/m^2] on the surface during impact stress tests are also known [22].

Current techniques [23] provide some plasma discharge properties that can be used in a method that results in a reduction of surface discharge in a device or apparatus. From the experimental projects published to date [12], [18], [20]-[21], [25]-[26], [29], this route appears to be an effective direction for the formation of layered materials at the dielectric interface and the formation of nanomaterial composites with a basis for a subsequent increase in the electric surface intensity of $E_{pt,\varepsilon}$.

3. ELECTRICAL SURFACE STRENGTH ADJUSTMENTS

Long-term durability testing of HV devices or HV equipment also includes a test of the effects of the ultimate electrical strength of the surface with an assessment of the wear/destruction of the insulator surface. Surface erosion can occur if the settings are incorrect, Fig. 4. To prevent such conditions, it is possible to numerically model the probability of erosion due to the long-term effect of the tangential component of the electrical intensity E_t [16] and set appropriate conditions in the design of the device. Another way to address this problem is to retrofit the insulator or its surface, Fig. 3.

Changes in the surface properties of insulators are assessed by measuring the surface resistance R_p and correlating it with the resistance to the tangential component of the electric field intensity E_t.

The evaluation and finding of the tangential component of the intensity is carried out by measuring the surface resistance R_p [Ω] and the residual surface electric charge σ [C/m^2]. In order to determine the effect of surface modifications, this measurement is performed before and after the application of the plasma discharge in a specific time interval t [s] (t = 24 h, t = 48 h, t = 72 h, t = 96 h, t = 120 h, t = 144 h).

Fig. 4. The effect of boundary surface electrical strength in the aging test process of HV electrical apparatus insulation material.

4. APPLICATION OF PLASMA FOR THE TREATMENT OF DIELECTRIC SURFACES

An atmospheric pressure plasma generation chamber in argon, argon-nitrogen or argon-oxygen atmosphere was numerically modeled and the electromagnetic field (EMF) distribution, electric *E*- and magnetic *H*-field intensity, power transfer and spectral distribution of these components in the frequency range f_1 = 13.56 MHz to 1 GHz were analyzed. The chamber was excited by a powerful HF generator with parametrically adjustable power P = 10-1000 W for the first harmonic f_1. Fig. 5 shows a real chamber and its schematic structure. The chamber generates a slit jet (PSJ) of plasma.

Fig. 6 shows the 3D model for the finite element analysis [13]-[14] in ANSYS, with most of the HFSS module included in the system. The boundary and initial conditions for the Hamonian nanolysis of the fundamental frequency component of the excitation chamber f = 13.56 MHz were defined. Fig. 7 shows the frequency characteristics of the chamber model when the plasma discharge is ignited using an experimentally verifiable, previously published method [26]. Fig. 8 and Fig. 9 interpret the distribution of the electric field strength modulus E and the magnetic field strength modulus H.

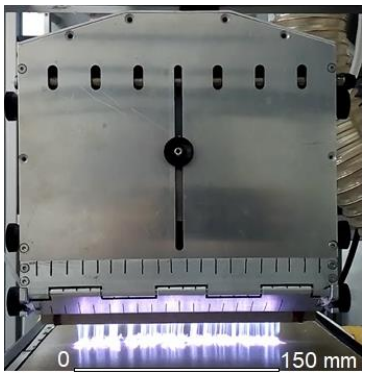

(a)

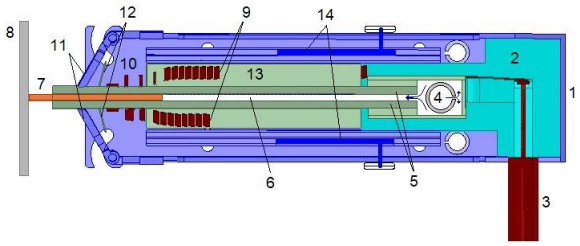

(b)

Fig. 5. Photo of the plasma chamber (a) and its schematic in cross section (b):

1. Shield cover (aluminum)
2. Supporting part made of PA6
3. Coaxial cable (50 Ω)
4. Argon flow homogenization
5. Mica composite plates (COGETHERM P)
6. Cavity (slot)
7. Plasma jet
8. Sample (dielectric plate)
9. Coil threads
10. High frequency electrode system (high voltage coil turns)
11. Folding ground electrode (part of the shield cover)
12. Dielectric plates of the environmental breakdown limiter
13. Support plates for coil turns (mica composite)
14. Sliding tuning plates (aluminum)

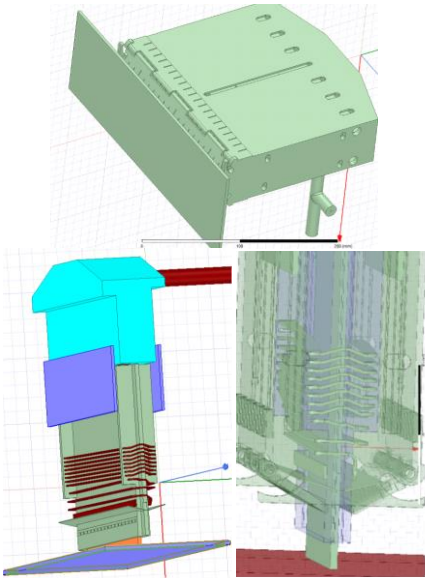

Fig. 6. The geometric model of the 3D PSJ, detail of the chamber section at its mouth, ANSYS HFSS system.

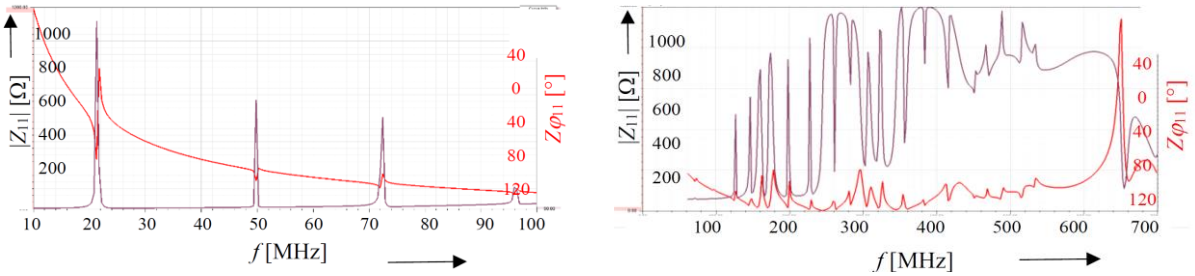

Fig. 7. Frequency analysis of the PSJ input transmission characteristics for the case of existence with plasma, developed in the numerical FEM model for the EMG field: (a) and (b) $|Z_{11}|$, $Z_{\varphi 11}$.

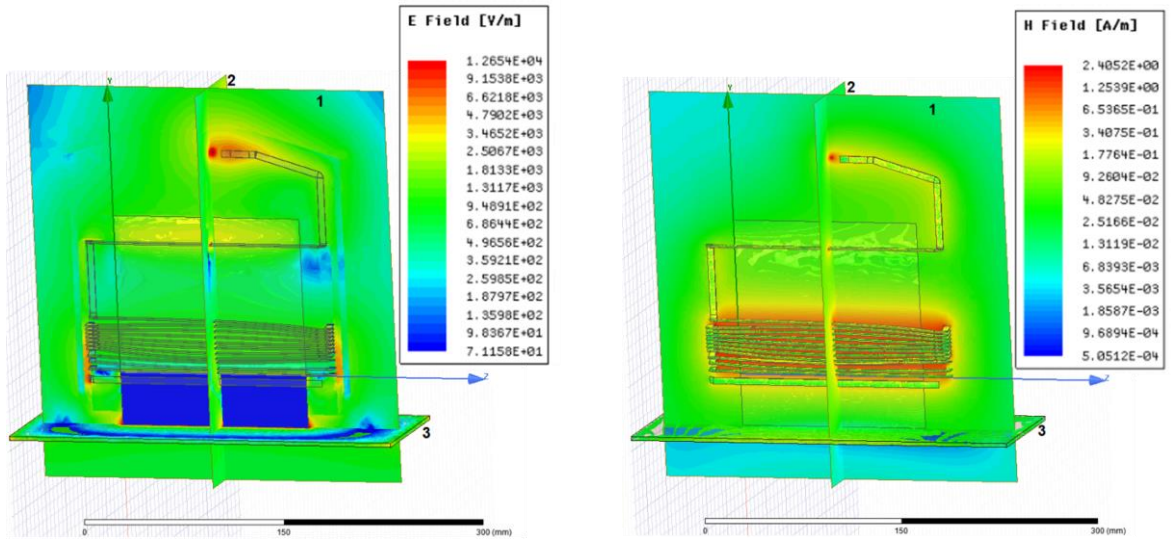

Fig. 8. The display of the EMG field quantities of a PSJ type plasma chamber for a power of P_{out} = 600 W and a frequency of f = 13.56 MHz (distance of the plasma chamber mouth of 10 mm from the dielectric material ε_r = 6, thickness of 3 mm, under which the plate is located): (a) electric field strength modulus and (b) magnetic field strength modulus.

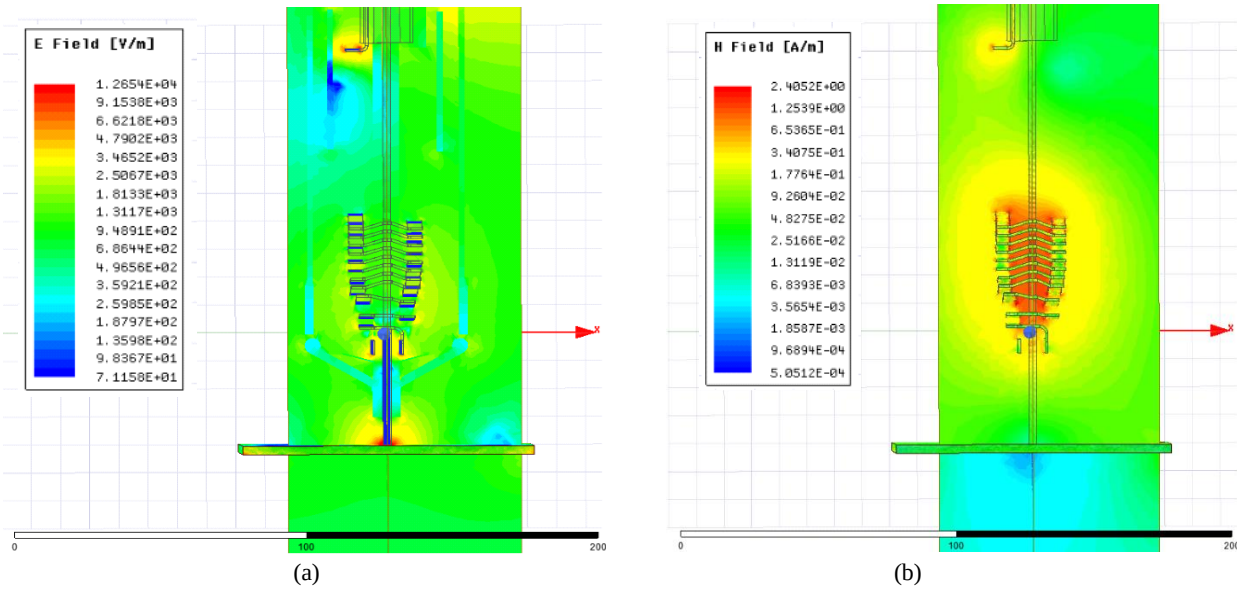

Fig. 9. Detail of the EMG field model of the PSJ type A plasma nozzle from Fig. 6 (plane 2): (a) electric field strength modulus, (b) magnetic field strength modulus.

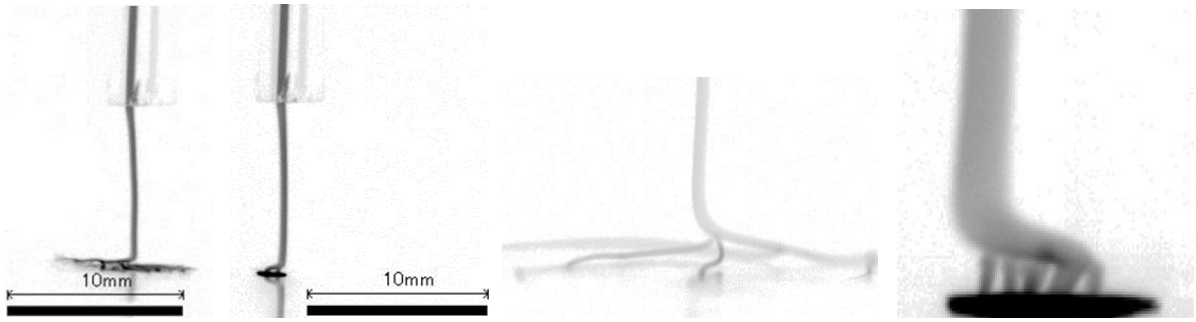

Fig. 10. Detail of the RF plasma discharge interacting with a substrate material with contrasting properties (metal, dielectric): (a) overall view of the discharge interacting with the dielectric substrate (ε_r = 6), (b) overall view of the discharge interacting with the metallic grounded substrate (aluminum), (c) detail of the plasma/plasma channels on the surface of the dielectric substrate (stable central plasma channel branching into relatively long side channels with high dynamics of expression), (d) detail of the discharge on the surface of the metallic grounded pad (stable central plasma channel that merges into the cathode plate in the form of many short plasma channels with extremely high dynamics of expression, Fig. 11.

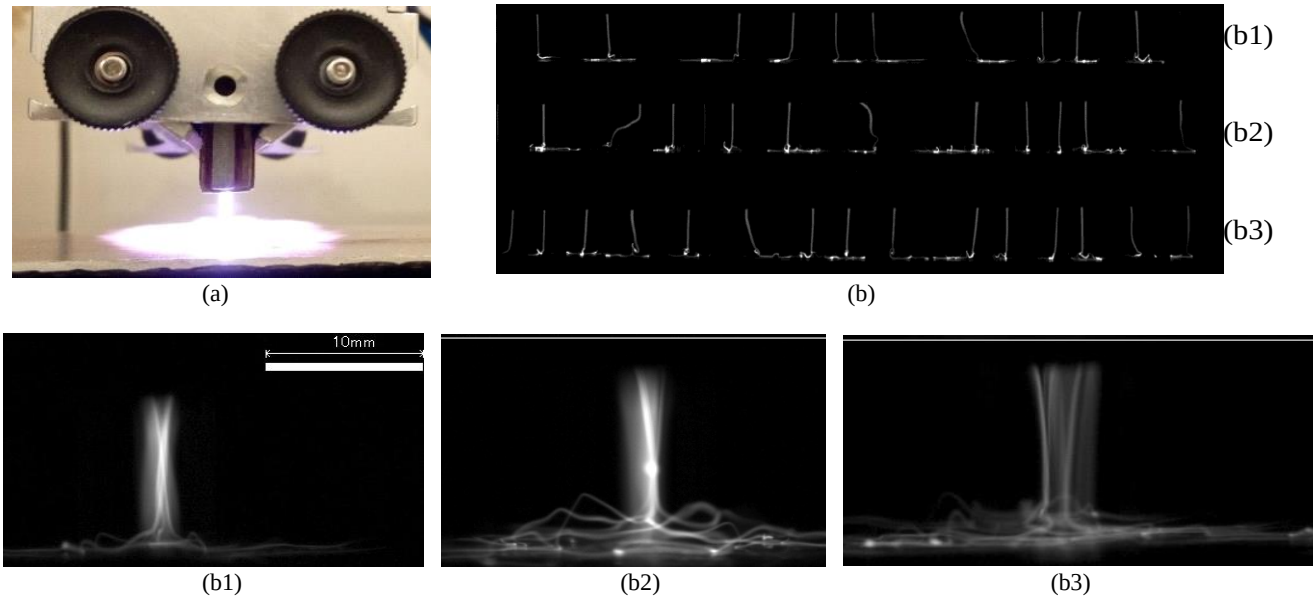

Fig. 11. Example for the comparison of the influence of the Ar flow rate and the power of the RF source on the number and dynamic behavior of the plasma channels at a plasma discharge slit width of 150 mm (a) side view, shutter speed 1/30 s, (b) side view (fast camera) for the plasma discharge mouth height of 10 mm above the dielectric pad (ε_r = 10) and the steady state (without pad movement): (b1) power P_{out} = 500 W, flow rate Ar w = 4 m^3/h, (b2) power P_{out} = 500 W, flow rate Ar w = 6 m^3/h, (b3) power P_{out} = 600 W, flow rate Ar w = 6 m^3/h.

The numerical model influences the boundary and initial conditions of the EMG field of plasma discharge generation and propagation. The numerical modeling and analysis were complemented by the experimental verification of the discharge and its evaluation, Fig. 10. Fig. 11. A fast camera was used to capture the discharge dynamics and the tests of the basic parameters were evaluated with respect to the desired influence on the surface dielectric of the test sample.

The first plasma discharge setup and the test of the effect on the dielectric samples were carried out using the parameters determined in this way.

5. METHODOLOGY FOR MEASURING AND EVALUATING SURFACE INTENSITY E_{PT}

The surface resistivity ρ_p (also surface resistance R_p) can be measured according to the recommendations of the standards [30], but it is not necessary to follow them strictly. For the first validation of the method, a device for evaluating the surface resistivity of the samples with a concentric ring probe and an electrometer (Keithley 6517A) was used, Fig. 12. The basic measured quantity is the determination of the surface resistivity R_p of the materials and the dimensions of the probe, which are r_1 = 12.2 mm, r_2 = 21.0 mm. Probe resistance R_s = 6.18406 .10^{11} Ω.

As the probe resistance R_s is of the same order of magnitude as the evaluated surface resistance R_p of the material sample under test, this condition must be considered when evaluating the surface resistance. An alternative circuit with resistors connected in parallel is shown in Fig. 13, from which the surface resistance of the sample R_p is determined:

$$\frac{1}{R_c} = \frac{1}{R_s} + \frac{1}{R_p} \tag{3}$$

where R_c is the total measured resistance. After the adjustment, the surface resistance is:

$$R_p = \frac{R_c \cdot R_s}{R_c - R_s} \tag{4}$$

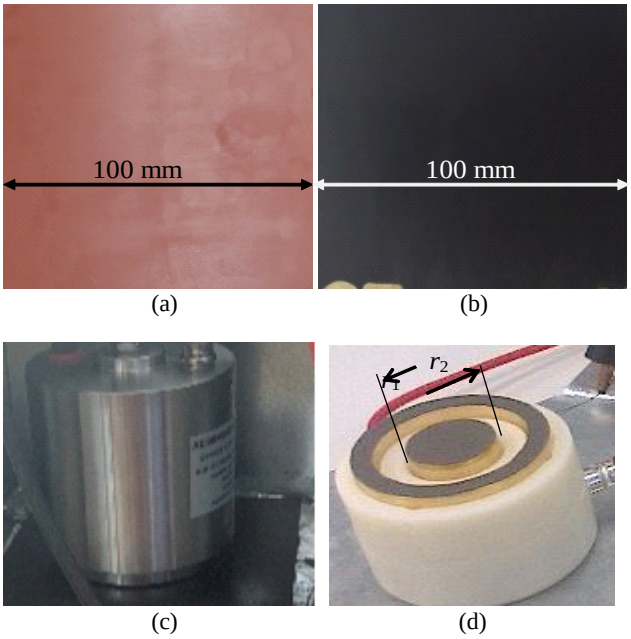

Fig. 12. Test samples of dielectric materials used for HV insulators: (a) epoxy base-thermoset type, (b) PE-thermoplastic base, (c) chamber and probe sample for measurement and evaluation of surface electric intensity E_{pt}, (d) geometrical arrangement of probe electrodes.

The relationship between the surface resistance R_p and the surface resistivity ρ_p can be found by determining the surface current density in the region between the rings of the circular probe. The electric field intensity E_p in the intermediate ring can be determined from knowledge of the surface current density J_p . Let us define r_1 as the radius of the inner electrode and r_2 as the inner radius of the outer ring electrode (Fig. 12(d)).

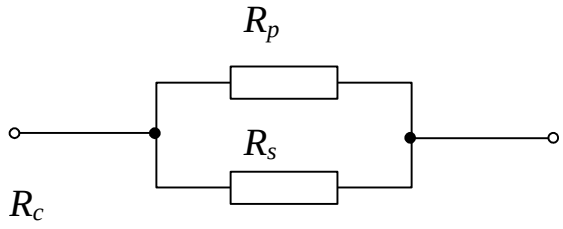

Fig. 13. Substitute schematic of the electrical arrangement of the sample resistors R_p and the characteristics of the measuring probe R_s.

Then the surface current density J_p [Am^{-1}] for the concentric ring probe is expressed as:

$$J_p = \frac{I_p}{2\pi r}, \tag{5}$$

where r is the distance between the electrodes with radii r_1 and r_2, I_p is the surface value of the electric current. It is assumed that when measuring the surface resistivity or resistivity in any material, the electric currents between the electrodes propagate along the surface and do not penetrate into the volume of the material. For this purpose, some more advanced techniques have been developed to measure surface resistivity [23]. for the following then applies to the current density J_p and the electric field intensity E_p:

$$J_p = \frac{E_p}{\rho_p}. \tag{6}$$

The surface electric field intensity between the concentric rings of the probe E_p, Fig. 12(d), can be determined using equations (3) and (4):

$$E_p = \frac{\rho_p I_p}{2\pi r}. \tag{7}$$

The electric voltage between the electrodes can be determined by integrating the electric field intensity E_p from r_1 to r_2:

$$U_{r_1,r_2} = \int_{r_1}^{r_2} E_p \, dr = \int_{r_1}^{r_2} \frac{\rho_p I_p}{2\pi r} dr = \frac{\rho_p I_p}{2\pi} \int_{r_1}^{r_2} \frac{1}{r} dr = \frac{\rho_p I_p}{2\pi} \ln\left(\frac{r_2}{r_1}\right). \tag{8}$$

After taking $R_p = U_{r1,r2}/I_p$ the following is true:

$$R_p = \frac{\rho_p}{2\pi} \ln\left(\frac{r_2}{r_1}\right). \tag{9}$$

After adjusting the relationship, it is clear that the difference between the surface resistivity and the surface resistance is only a constant that depends on the geometry of the electrodes:

$$\rho_p = R_p \frac{2\pi}{\ln\left(\frac{r_2}{r_1}\right)} = R_p \cdot k, \tag{10}$$

where k is the coefficient of the probe geometry [24].

A. Detailed description of the plasma surface treatment

The plasma (in the argon atmosphere) is generated using a system consisting of a power HF generator and a plasma chamber. The chamber generates the slit jet - PSJ, the effective area of the plasma jet is 150 mm. The plasma is generated with a flow rate of w = 4 m^3/h of gas (argon). The high-frequency power generator to produce PSJ has an operating frequency of the first harmonic at f_1 = 13.56 MHz and the output is regulated to a power of up to P_{out} = 600 W.

In the pilot test series for surface treatment of dielectric samples (6 samples, 2 control measurements), the power was set to P_{out} = 500 W, Fig. 14(a). The repeatability of the plasma effect on the sample was ensured by an automated feed with a set constant feed rate. The samples and their surfaces were repeatedly (twice) subjected to plasma amples were exposed, while 2 pc of the samples were left unexposed to compare the measured parameters, Fig. 7(b). The distance of the mouth of the plasma nozzle from the sample surface was micrometrically adjusted to d = 10.0 mm.

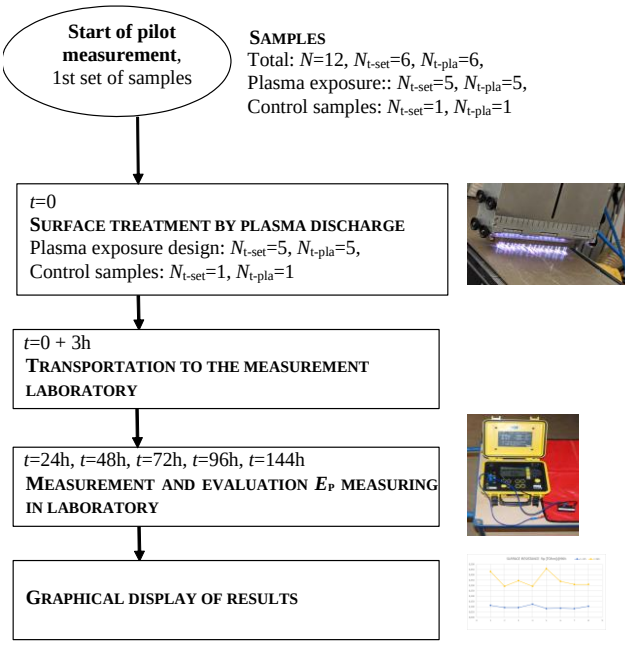

(a)

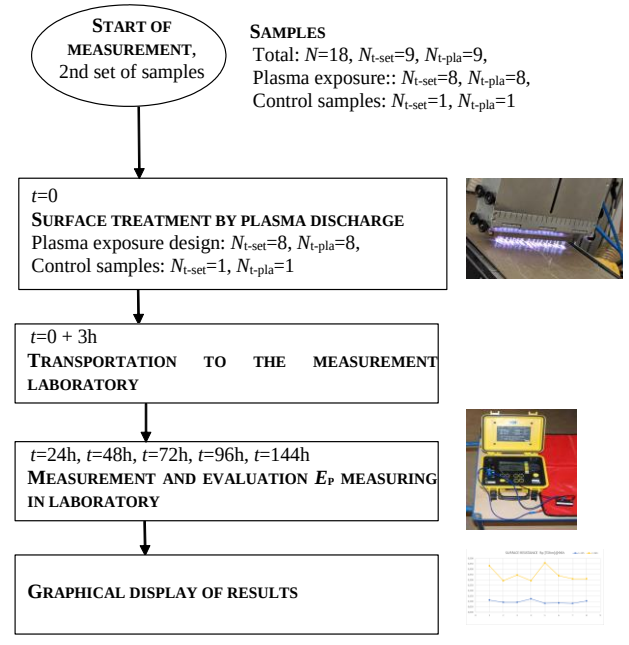

(b)

Fig. 14. Schematic representation of the measurement process and the verification of the parameters of the tested dielectric samples, (a) pilot measurement for the 1st set of samples, (b) measurement for the 2nd set of samples.

B. Surface treatment and measuring methodologies

The test methodology [26]-[28] and the relevant parameters were verified as follows (Fig. 14):

1. In the first step, the proposed methodology was used to measure a pair of 6 pc samples, two of which were without surface treatment. The treatment was performed on samples of both material types.
2. After verifying the parameters and repeatability of the discharge exposure, the procedure was performed again, this time on 18 pc samples of both material types.
3. Before and after the sample surface was exposed to the plasma discharge, the following was measured and evaluated: the residual surface electric charge σ [C/m^2], the surface resistance R_p [Ω], and the electric current flowing through the sample I_s [μA], the evaluated electric field intensities on the sample surface E_{pt} [V/m].
4. The time dependence of the stability of the parameters R_p, I_s, E_{pt} was monitored and the measurement according to point 2 was repeated at predefined time intervals T, namely 24 h, 48 h, 72 h, and 120 h to 144 h after exposure to the plasma discharge.
5. Post-exposure samples were transported in a container with defined material and surface conductivity, predefined dimensions and material structure/ composition. The electric surface charge of the transport boxes was measured and adjusted to ensure a minimum surface charge of the exposed sample during storage and transportation to the measurement laboratory.

The parameters of the samples after exposure were measured according to the above methodology with the following steps:

a. Calibration of the measuring system: device, probe, environment, unexposed sample,
b. Measurement and evaluation of the resistance R_c with CA-6543,
c. Simultaneous measurement of the electric current with a Kethley probe,
d. Evaluation of the resistance R_v, the electric surface charge density σ and the electric field intensity E_p in exposed and unexposed samples,
e. The entire procedure 1-4 was repeated for the interval T = 24 h, 48 h, 72 h, and 120 h to 144 h,
f. Evaluation of the measured data and graphical recording.

Based on the measurement methodology described above, the evaluation of the time dependence of the observed treatment parameters and the verification of the influence of the surface conductivity/resistance of the insulator sample and the magnitude of the electric field intensity E_p are shown graphically in Fig. 15 and Fig. 16.

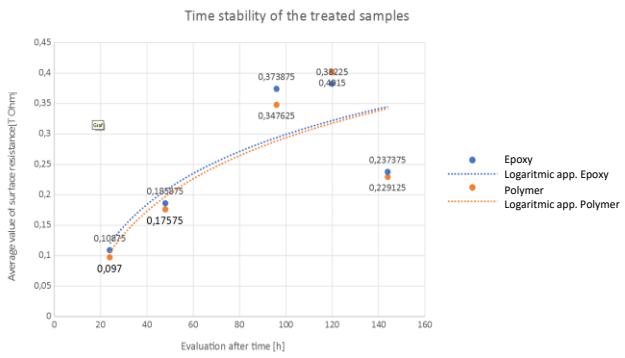

Fig. 15. Evaluation of the time stability of the first series of samples treated with argon plasma (N = 16) of both types of plastic (epoxy-based, polymer-based).

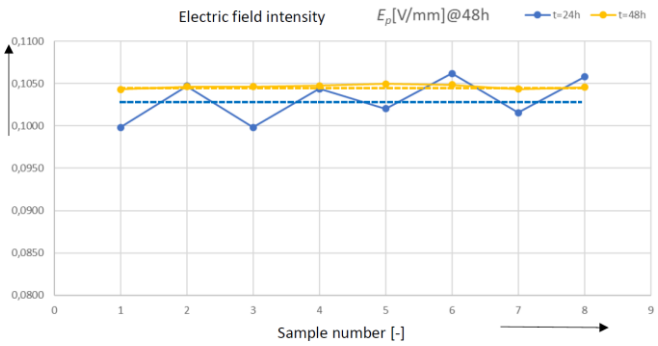

(a)

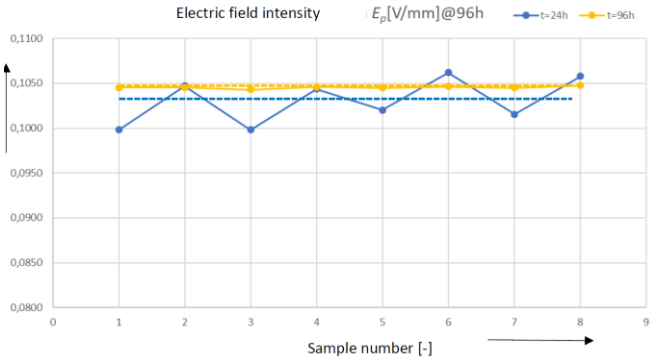

(b)

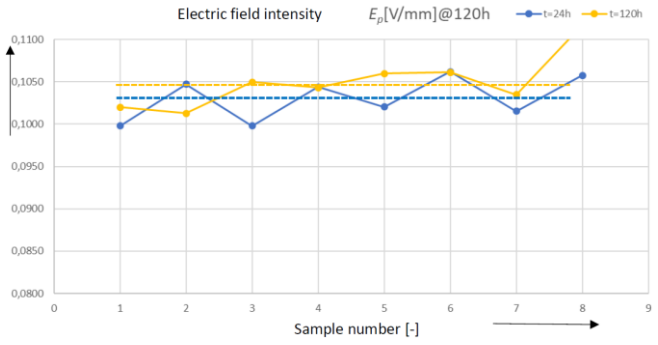

(c)

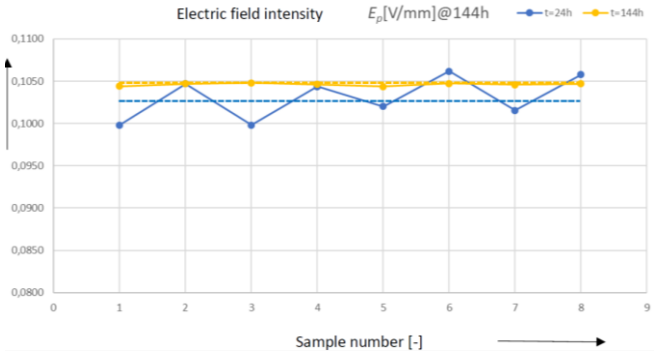

(d)

Fig. 16. Evaluation of the electric surface intensity E_{pt} as a function of the measurement from the time of plasma surface treatment (a) t = 48 h, (b) t = 96 h, (c) t = 120 h, (d) t = 144 h); thermoset sample (the dashed value is the evaluated average value of the quantity).

6. RESULTS

Using the measurement methodology described, the data evaluation was performed with a partial graphical representation of the evaluation of the dependence of the observed treatment parameters on time and the verification of the change in the surface conductivity/resistivity, the electrical strength E of the insulator sample. A generator with an output power of P_{out} = 10-1000 W, U_{out} = 300-600 V, periodic signal and first harmonic f_1 = 13.56 MHz was used for the plasma treatment. The evaluations of the measured parameters can be found in Table 1 and Table 2.

Graphical waveforms of the changes in the measured parameters, Fig. 8, and the subsequently evaluated electric surface strengths of the insulator samples as a function of time (from the exposure time without precursor) are shown in Fig. 16. The surface resistance of the untreated samples of the second series of materials was $R_{p,tset}$ = 0.082 TΩ and $R_{p,tplast}$ = 0.092 TΩ. Plasma surface treatment without precursors shows that the surface resistance R_p for thermoplastic materials and thermosets increases and does not decrease with time, but stabilizes at higher values, Fig. 15. Further research will focus on the selection and use of precursors; the effects on surface resistance R_p and its stability over time will also be investigated.

7. DISCUSSION

The methodology described and the exemplary implementation of repeated plasma exposure on the surface of a dielectric material have shown that a nanometer-scale change in the surface can influence the surface electrical strength. The methodology and process were chosen with regard to the intended application of the method in industrial use in the manufacture of HV and MV equipment. In this production process, the surfaces cannot be specially chemically prepared for plasma treatment for economic reasons, nor can they be treated over longer periods of time. The samples of the tested materials were therefore prepared with this in mind. It was also necessary to consider the subsequent process in the manufacture of the devices, where the device cannot be stored for long periods and somehow packaged in special packaging materials.

Therefore, the methodology pays more attention to the residual electric charge on the surface of the dielectric after plasma treatment. This part will be closely monitored in future measurements. The first measurements and sample manipulations [12] have shown that the surface charge can influence the resulting evaluated electric field intensity jump parameter.

Table 1 and Table 2 show the measurements by time interval. They show that the sample manipulation can influence the measurement and its result. It was evident in the measurement and evaluation after 140 hours due to the influence of the plasma, Fig. 15.

Table 1. Measurement I - first set of samples - Measurement and evaluation of dielectric material samples by plasma discharge.

Measurement I

	to 24 h		to 48 h		to 96 h		to 120 h		to 144 h	
Timeline	R_p	I_s	R_p	I_s	R_p	I_s	R_p	I_s	R_p	I_s
Sample	TΩ	nA	TΩ	nA	TΩ	nA	TΩ	nA	TΩ	nA
*E1	0.128	3.834	0.179	2.791	0.339	1.473	0.407	1.252	0.259	1.925
E2	0.082	5.958	0.175	2.855	0.489	1.022	0.345	1.414	0.219	2.280
E3	0.123	3.995	0.173	2.887	0.344	1.455	0.328	1.510	0.228	2.193
E4	0.119	4.295	0.159	3.187	0.342	1.510	0.321	1.628	0.238	1.981
E5	0.109	4.531	0.169	2.951	0.325	1.538	0.295	1.765	0.295	1.695
E1	0.092	5.439	0.155	3.226	0.293	1.705	0.413	1.172	0.215	2.327
E2	0.124	4.023	0.168	2.980	0.293	1.706	0.397	1.256	0.295	1.695
E3	0.086	5.901	0.216	2.320	0.339	1.475	0.438	1.158	0.208	2.406
E4	0.105	4.861	0.218	2.282	0.310	1.610	0.439	1.149	0.202	2.489
E5	0.104	4.986	0.219	2.081	0.311	1.584	0.442	1.087	0.201	2.521
Avg.	0.140		0.214		0.460		0.424		0.310	
Avg.	0.128		0.244		0.387		0.532		0.280	

*E … epoxy

Table 2. Measurement II - second set of samples - Measurement and evaluation of dielectric material samples by plasma discharge.

Measurement II

	to 24 h			to 48 h			to 96 h			to 120 h			to 144 h		
Timeline	R_p	I_s	E	R_p	I_s	E	R_p	I_s	E	R_p	I_s	E	R_p	I_s	E
Sample	TΩ	nA	V/mm	TΩ	nA	V/mm	TΩ	nA	V/mm	TΩ	nA	V/mm	TΩ	nA	V/mm
*TP1	0.082	6.085	0.1044	0.245	2.033	0.1042	0.357	1.333	0.0996	0.497	1.084	0.1127	0.265	1.886	0.1046
TP2	0.128	3.834	0.1027	0.179	2.791	0.1045	0.339	1.473	0.1044	0.407	1.252	0.1066	0.259	1.925	0.1043
TP3	0.108	4.762	0.1076	0.165	3.019	0.1042	0.441	1.135	0.1047	0.327	1.782	0.1219	0.224	2.236	0.1048
TP4	0.082	5.958	0.1022	0.175	2.855	0.1045	0.489	1.022	0.1046	0.345	1.414	0.1021	0.219	2.280	0.1045
TP5	0.112	4.543	0.1065	0.202	2.476	0.1047	0.382	1.308	0.1045	0.402	1.326	0.1115	0.174	2.879	0.1048
TP6	0.123	3.995	0.1028	0.173	2.887	0.1045	0.344	1.455	0.1047	0.328	1.510	0.1036	0.228	2.193	0.1046
TP7	0.126	4.038	0.1065	0.179	2.800	0.1049	0.314	1.592	0.1046	0.457	1.184	0.1132	0.235	2.125	0.1045
TP8	0.109	4.531	0.1033	0.169	2.951	0.1044	0.325	1.538	0.1046	0.295	1.765	0.1089	0.295	1.695	0.1046
**EP1	0.113	4.221	0.0998	0.163	3.058	0.1043	0.431	1.159	0.1045	0.340	1.434	0.1020	0.256	1.949	0.1044
EP2	0.092	5.439	0.1047	0.155	3.226	0.1046	0.293	1.705	0.1045	0.413	1.172	0.1013	0.215	2.327	0.1047
EP3	0.092	5.185	0.0998	0.153	3.268	0.1046	0.345	1.445	0.1043	0.427	1.175	0.1050	0.241	2.078	0.1048
EP4	0.124	4.023	0.1044	0.168	2.980	0.1048	0.293	1.706	0.1046	0.397	1.256	0.1043	0.295	1.695	0.1046
EP5	0.083	5.875	0.1020	0.161	3.115	0.1049	0.459	1.088	0.1045	0.434	1.167	0.1060	0.196	2.545	0.1044
EP6	0.086	5.901	0.1062	0.216	2.320	0.1049	0.339	1.475	0.1046	0.438	1.158	0.1061	0.208	2.406	0.1047
EP7	0.082	5.918	0.1015	0.171	2.916	0.1043	0.310	1.611	0.1045	0.321	1.541	0.1035	0.221	2.262	0.1046
EP8	0.104	4.861	0.1058	0.219	2.282	0.1046	0.311	1.610	0.1048	0.442	1.208	0.1117	0.201	2.489	0.1047
Avg.	0.109			0.186			0.374			0.382			0.237		
Avg.	0.097			0.176			0.348			0.402			0.229		

*TP ... thermoplastic **EP ... epoxy

8. Conclusion

The proposed method for measuring and evaluating the effects of plasma surface treatment of the dielectric/insulator was piloted and repeatedly verified on sets of test samples. The reproducibility and the expected change (increase) in surface electric strength after plasma exposure were demonstrated; the effects and quantitative change were graphically represented. The method showed that plasma treatment demonstrably and reproducibly increases the surface intensity parameters of the dielectric (and thus the resistance to overshoot) for both thermoset and thermoplastic dielectrics in the order of tens of percent. The contribution of the research lies in the systematic, technologically manageable exposure and evaluation of insulator surfaces, which is clearly industrially applicable. The next phases of the research will test the use of suitable precursors in plasma and evaluate their effect on key dielectric properties in order to refine the surface property parameters of insulators, complemented by measurable documentation of radio spectra as indicators of changes in the surface properties of insulators.

Acknowledgment

The research was funded under the National Sustainability Program, a grant from the Czech Science Foundation (GA 20-14105S) and grants BD 2020-2022, FEKT-S-20-6360. BD 2023-2025, FEKT-S-23-8425.

References

[1] Kikuchi, H. (2001). *Electrohydrodynamics in Dusty and Dirty Plasmas: Gravito-Electrodynamics and EHD*. Springer, 227. ISBN 978-0792368229.

[2] Fridman, A. (2008). *Plasma Chemistry*. Cambridge University Press. ISBN 978-0511546075. https://doi.org/10.1017/CBO9780511546075

[3] Drexler, P., Fiala, P., Klima, M., Szabó, Z., Dostál, L., Kadlec, R., Pernica, R. (2021). Electromagnetic modeling of a plasma chamber: Theory and experiments. In *2021 Photonics & Electromagnetics Research Symposium (PIERS)*. IEEE. https://doi.org/10.1109/PIERS53385.2021.9694874

[4] Koinuma, H., Ohkubo, H., Hashimoto, T., Inomata, K., Shiraishi, T., Miyanaga, A., Hayashiet, S. (1992). Development and application of a microbeam plasma generator. *Applied Physics Letters*, 60 (7), 816-817. https://doi.org/10.1063/1.106527

[5] Klíma, M., Zajíková, L., Jana, J. (1997). The perspectives of plasmachemical treatment on ancient artifacts. *Zeitschrift für Schweizerische Archäologie und Kunstgeschichte*, 54, 31-33. http://dx.doi.org/10.5169/seals-169507

[6] Raballand, V., Benedikt, J., von Keudell, A. (2008). Deposition of carbon-free silicon dioxide from pure hexamethyldisiloxane using an atmospheric microplasma jet. *Applied Physics Letters*, 92 (9), 091502. https://doi.org/10.1063/1.2844880

[7] Schäfer, J., Fricke, K., Mika, F., Pokorná, Z., Zajíčková, L., Foest, R. (2017). Liquid assisted plasma enhanced chemical vapour deposition with a non-thermal plasma jet at atmospheric pressure. *Thin Solid Films*, 630, 71-78. https://doi.org/10.1016/j.tsf.2016.09.022

[8] Beijer, P. A. C., Sobota, A., van Veldhuizen, E. M., Kroesen, G. M. W. (2016). Multiplying probe for accurate power measurements on an RF driven atmospheric pressure plasma jet applied to the COST reference microplasma jet. *Journal of Physics D: Applied Physics*, 49 (10), 104001. https://doi.org/10.1088/0022-3727/49/10/104001

[9] Klíma, M., Janča, J., Kapička, V., Slavíček, P., Saul, P. (2000). *Způsob vytváření fyzikálně a chemicky aktivního prostředí plazmovou tryskou a plazmová tryska (Method of making a physically and chemically active environment by means of a plasma jet and the related plasma jet)*. Patent CZ286310 (2000), US6525481B1 (2003), EP1077021A1 (2005).

[10] Klíma, M., Slavíček, P., Šíra, M., Čižmár, T., Vaněk, P. (2006). HF plasma pencil and DC diaphragm discharge in liquids - diagnostics and application. *Czechoslovak Journal of Physics*, 56, B1051-B1056. https://doi.org/10.1007/s10582-006-0325-x

[11] Yablokov, M., Gilman, A., Kuznetsov, A. (2017). Modification of wettability of polymer surfaces by plasma. In *Proceedings of the 21st Symposium on Application of Plasma Processes*. Bratislava, SK: Comenius University Bratislava, 19-26.

[12] Pernica, R., Klíma, M., Londák, P., Fiala, P. (2024). Modification of insulating properties of surfaces of dielectric high-voltage devices using plasma. *Applied Sciences*, 14 (11), 4399. https://doi.org/10.3390/app14114399

[13] Stratton, J. A. (2007). *Electromagnetic Theory*. Wiley, ISBN 9780470131534.

[14] ANSYS, Inc., https://www.ansys.com/

[15] Kopeček, J., Dvořák, M. (1966). *Přístrojové transformátory*. Praha, ČR: Academia.

[16] Fiala, P. (1999). *Modelování transformátoru proudu při zkratu (Modeling of current transformers on a short-circuit)*. PhD Thesis, VUT FEI, Brno, ČR. ISBN 80-214-1346-8.

[17] Havelka, O. a kol. (1985). *Elektrické přístroje*. Praha, ČR: SNTL. ISBN 04-529-85.

[18] Lin, L., Rui, L., Tao, Y., Li, Q., Chiang, W.-H., Xu, H. (2022). Surface modification of metal substrates using dielectric barrier discharge plasma and the wettability study. *Journal of the Taiwan Institute of Chemical Engineers*, 138, 104467. https://doi.org/10.1016/j.jtice.2022.104467

[19] Kříž, M. (2019). *Dimenzování a jištění elektrických zařízení*. Pardubice, ČR: IN-EL. ISBN 9788087942482.

[20] Sujar-Garrido, P., Becerra, M., Örlü, R. (2022). Efficiency assessment of a single surface dielectric barrier discharge plasma actuator with an optimized Suzen-Huang model. *Physics of Fluids*, 34 (4), 047110. https://doi.org/10.1063/5.0087395

[21] Wang, C.. Zhang, G., Wang, X., He, X. (2010). The effect of air plasma on barrier dielectric surface in dielectric barrier discharge. *Applied Surface Science*, 257 (5), 1698-1702. https://doi.org/10.1016/j.apsusc.2010.08.125

[22] Deng, J., Matsuoka, S., Kumada, A., Hidaka, K., Pu, L., Zhang, G. (2012). Effect of residual charges on surface discharge propagation under impulse voltage. *Gaodianya Jishu/High Voltage Engineering*, 38 (8), 2137-2144. https://doi.org/10.3969/j.issn.1003-6520.2012.08.045

[23] Polášková, K., Nečas, D., Dostál, L., Klíma, M., Fiala, P., Zajíčková, L. (2022). Self-organization phenomena in cold atmospheric pressure plasma slit jet. *Plasma Sources Science and Technology*, 31, 125014. https://doi.org/10.1088/1361-6595/acab82

[24] Maryniak, W. A., Uehara, T., Noras, M. A. (2003). *Surface resistivity and surface resistance measurements: Using a concentric ring probe technique*. Trek Application Note 1005.

[25] Liang, H., Du, B., Li, J., Du, Q. (2018). Numerical simulation on the surface charge accumulation process of epoxy insulator under needle-plane corona discharge in air. *IET Science, Measurement and Technology*, 12 (1), 9-16. https://doi.org/10.1049/iet-smt.2017.0164

[26] Drexler, P. Szabó, Z., Pernica, R., Zukal, J., Kadlec, R., Klíma, M., Fiala, P. (2022). Modeling and experimental verification of plasma jet electromagnetic signals. *Modelling*, 3 (1), 70-91. https://doi.org/10.3390/modelling3010005

[27] Polášková, K., Ozkan, A., Klíma, M., Jeníková, Z., Buddhadasa, M., Reniers, F., Zajíčková, L. (2023). Comparing efficiencies of polypropylene treatment by atmospheric pressure plasma jets. *Plasma Processes and Polymers*, 20 (11), e2300031. https://doi.org/10.1002/ppap.202300031

[28] Polášková, K., Klíma, M., Jeníková, Z., Blahová, L., Zajíčková, L. (2021). Effect of low molecular weight oxidized materials and nitrogen groups on adhesive joints of polypropylene treated by a cold atmospheric plasma jet. *Polymers*, 13 (24), 4396. https://doi.org/10.3390/polym13244396

[29] Tian, L., Shen, L., Xue, Y., Chen, L., Li, L., Chen, P., Tian, J., Zhao, W. (2022). Theoretical and experimental research on spatial performances of the long-slit streak tube. *Measurement Science Review*, 22 (2), 58-64. https://doi.org/10.2478/msr-2022-0007

[30] ASTM. (1999). *Standard test methods for DC resistance or conductance of insulating materials*. Standard D 257-99.

Received May 3, 2024
Accepted November 26, 2024